Sussex Research Online

The origin of the most massive black holes at high-z: BlueTides and the next quasar frontier

Article (Published Version)

Di Matteo, Tiziana, Croft, Rupert A C, Feng, Yu, Waters, Dacen and Wilkins, Stephen (2017) The origin of the most massive black holes at high-z: BlueTides and the next quasar frontier. Monthly Notices of the Royal Astronomical Society, 467 (4). pp. 4243-4251. ISSN 0035-8711

This version is available from Sussex Research Online: http://sro.sussex.ac.uk/id/eprint/68373/

This document is made available in accordance with publisher policies and may differ from the published version or from the version of record. If you wish to cite this item you are advised to consult the publisher's version. Please see the URL above for details on accessing the published version.

Copyright and reuse:
Sussex Research Online is a digital repository of the research output of the University.

Copyright and all moral rights to the version of the paper presented here belong to the individual author(s) and/or other copyright owners. To the extent reasonable and practicable, the material made available in SRO has been checked for eligibility before being made available.

Copies of full text items generally can be reproduced, displayed or performed and given to third parties in any format or medium for personal research or study, educational, or not-for-profit purposes without prior permission or charge, provided that the authors, title and full bibliographic details are credited, a hyperlink and/or URL is given for the original metadata page and the content is not changed in any way.

http://sro.sussex.ac.uk

Monthly Notices
of the
ROYAL ASTRONOMICAL SOCIETY

MNRAS **467,** 4243–4251 (2017)
Advance Access publication 2017 February 9

doi:10.1093/mnras/stx319

The origin of the most massive black holes at high-z: BLUETIDES and the next quasar frontier

Tiziana Di Matteo,[1⋆] Rupert A. C. Croft,[1⋆] Yu Feng,[2] Dacen Waters[1] and Stephen Wilkins[3]

[1]*McWilliams Center for Cosmology, Physics Department, Carnegie Mellon University, Pittsburgh, PA 15213, USA*
[2]*Berkeley Center for Cosmological Physics, University of California at Berkeley, Berkeley, CA 94720, USA*
[3]*Astronomy Centre, Department of Physics and Astronomy, University of Sussex, Brighton BN1 9QH, UK*

Accepted 2017 February 2. Received 2017 February 2; in original form 2016 July 5

ABSTRACT

The growth of the most massive black holes in the early Universe, consistent with the detection of highly luminous quasars at $z > 6$ implies sustained, critical accretion of material to grow and power them. Given a black hole (BH) seed scenario, it is still uncertain which conditions in the early Universe allow the fastest BH growth. Large-scale hydrodynamical cosmological simulations of structure formation allow us to explore the conditions conducive to the growth of the earliest supermassive BHs. We use the cosmological hydrodynamic simulation BLUETIDES, which incorporates a variety of baryon physics in a $(400\,h^{-1}\mathrm{Mpc})^3$ volume with 0.7 trillion particles to follow the earliest phases of BH critical growth. At $z = 8$ the most massive BHs (a handful) approach masses of $10^8\,\mathrm{M}_\odot$ with the most massive (with $M_{\rm BH} = 4 \times 10^8\,\mathrm{M}_\odot$) being found in an extremely compact (compared to present day) spheroid-dominated host galaxy. Examining the large-scale environment of hosts, we find that the initial tidal field is more important than overdensity in setting the conditions for early BH growth. In regions of low tidal fields gas accretes 'cold' on to the BH and falls along thin, radial filaments straight into the centre forming the most compact galaxies and most massive BHs at the earliest times. Regions of high tidal fields instead induce larger coherent angular momenta and influence the formation of the first population of massive compact discs. The extreme early growth depends on the early interplay of high gas densities and the tidal field that shapes the mode of accretion. Mergers may play a minor role in the formation of the first generation, rare massive BHs.

Key words: black hole physics – methods: numerical – galaxies: formation – galaxies: high-redshift – early Universe – large-scale structure of Universe.

1 INTRODUCTION

One of the most challenging question for galaxy formation theory is to explain the observations of the first ($z = 6$) quasars in the Sloan Digital Sky Survey (SDSS; Fan et al. 2006; Jiang et al. 2009) and more recently the highest redshifts quasar discovered at $z \sim 7$ (Mortlock et al. 2011). Although rare, these objects imply that billion solar mass black holes (BHs) (similar to the most massive black holes today) must be assembled within the first eight hundred million years of the big bang. In the coming decade, a new generation of astronomical instruments, including some which are specifically targeting this epoch as their highest priority (the NASA *James Webb Space Telescope*) and also *Wide-Field Infrared Survey Telescope* (*WFIRST*), will start making observations of the Universe during the period of the first stars and quasars, and opening up the 'last frontier' in astronomy and cosmology.

Detailed theoretical predictions for these early times are hard to make, particularly those with the dynamic range to cover both the formation of individual objects and make statistical studies of them. Much recent work in galaxy formation focusing on early BH growth has involved carrying out 'zoomed' simulations (e.g. Dubois et al. 2012), where the full physics algorithms are only brought to bear on very small sub-volumes of larger simulations. This approach is well suited to modelling, the detailed dynamics of the inflowing cold gas as it falls to the centres of haloes, feeding the growth of the central supermassive BH. It is not possible, however, to use these simulations to make predictions for the statistics of the population of early BHs or to give information on the abundance of such rare objects. Luckily, large-scale uniform volume cosmological hydrodynamic simulation of the high-redshift Universe is a problem, which is suited to the largest modern supercomputers.

⋆ E-mail: tiziana@phys.cmu.edu (TDM); rcroft@cmu.edu (RACC)

© 2017 The Authors
Published by Oxford University Press on behalf of the Royal Astronomical Society

This means that it has now become feasible to reach unprecedented combinations of volume and resolution in the early Universe.

Here, we present a physical picture for the emergence of the most massive BHs at early times using the BlueTides simulation. As bright quasars are likely to occur in extremely rare high-density peaks in the early Universe, large computational volumes are needed to study them. In Di Matteo et al. (2012), we used the MassiveBlack simulation, a cosmological hydrodynamic simulation covering a volume $(0.75\,\mathrm{Gpc})^3$ appropriate for studying the rare first quasars to show that steady high-density cold gas flows responsible for assembling, the first galaxies produce the high gas densities that lead to sustained critical accretion rates and hence rapid growth commensurate with the existence of $\sim 10^9\,\mathrm{M}_\odot$ BHs as early as $z \sim 7$. Here we use our newest, higher resolution cosmological hydrodynamic simulation, BlueTides (Feng et al. 2015, 2016; Waters et al. 2016a,b) (covering a volume of $[0.5\,\mathrm{Gpc}]^3$) which includes improved prescriptions for star formation, as well as BH accretion and associated feedback processes. We focus on earlier times, searching for the conditions that allow rapid growth of the massive BHs beyond currently observed redshifts ($z > 7$). This also allows us to make predictions for the most massive BHs to be discovered in the near future. Large volume simulations such as *MassiveBlack* (Di Matteo et al. 2012) and associated high-resolutions zooms (Feng et al. 2014) already showed that the existence of the $z = 6$ SDSS quasar population is consistent with our standard structure formation models. Crucially, the BlueTides simulation with its increased resolution, allows us to study reliably the formation of massive BHs at even earlier times. It therefore provides a unique framework to study the formation of the next frontier of even higher redshift quasars that soon will be discovered with NASA *James Webb Space Telescope* and *WFIRST*.

2 BlueTides SIMULATION

The BlueTides simulation (see Feng et al. 2015, 2016 for a full description) was carried out using the Smoothed Particle Hydrodynamics code MP-GADGET with 2×7040^3 particles on the Blue Waters system at the National Centre for Supercomputing Applications. The simulation evolved a $(400\,h^{-1})^3\,\mathrm{cMpc}^3$ cube to $z = 8$ by which time it contained approximately 200 million objects (of which 160000 have stellar masses greater than $10^8\,\mathrm{M}_\odot$). The dark matter and gas particle masses are $M_{\rm DM} = 1.2 \times 10^7\,h^{-1}\,\mathrm{M}_\odot$, $M_{\rm Gas} = 2.36 \times 10^6\,h^{-1}\,\mathrm{M}_\odot$, respectively. The gravitational smoothing length is $1.5\,h^{-1}$ kpc. At $z = 10$ the number of objects identified falls to around 20 million, and only around 30000 have stellar masses greater than $10^{10}\,\mathrm{M}_\odot$. The galaxy stellar mass and rest-frame ultraviolet (UV) luminosity functions predicted by the simulation (Feng et al. 2015, 2016; Waters et al. 2016a; Wilkins et al. 2016a,b) match observational constraints available at $z = 8$, 9 and 10 (e.g Bouwens et al. 2015; Song et al. 2016). The large volume of BlueTides, almost 200 times larger than either the Illustris (Vogelsberger et al. 2014) or EAGLE (Schaye et al. 2015) simulations, makes it ideally suited to an investigation of rare objects at high redshift. The high resolution (comparable to Illustris) also allows the study of the formation of the first massive galaxies and details of the structure and gas inflows inside galaxies. BlueTides was run assuming a cosmology consistent with the *Wilkinson Microwave Anisotropy Probe* nine year data release (Hinshaw et al. 2013). The simulation is described in more detail in Feng et al. (2015, 2016), while the physical and observed properties of the galaxy population and predictions for the BH active galactic nucleus (AGN) population and luminosity functions are described in detail in Feng et al. (2015, 2016), Waters et al. (2016a,b) and Wilkins et al. (2016b,c). To produce galaxy photometry, we assume a Chabrier (2003) initial mass function and use the Pegase.2 stellar population synthesis model (Fioc & Rocca-Volmerange 1997).

A variety of sub-grid physical processes were implemented to study their effects on galaxy formation:

(i) star formation based on a multiphase star formation model (Springel & Hernquist 2003) with modifications following Vogelsberger et al. (2013);
(ii) gas cooling through radiative processes (Katz, Weinberg & Hernquist 1996) and metal cooling (Vogelsberger et al. 2014);
(iii) formation of molecular hydrogen and its effects on star formation (Krumholz & Gnedin 2011);
(iv) Type II supernovae wind feedback (the model used in Illustris Nelson et al. 2015);
(v) BH growth and AGN feedback using the same model as in MassiveBlack I and II (Di Matteo, Springel & Hernquist 2005);
(vi) a model of 'patchy' reionization (Battaglia et al. 2013) yielding a mean reionization redshift $z \approx 10$ (Hinshaw et al. 2013), and incorporating the UV background estimated by Faucher-Giguère et al. (2009).

In Feng et al. (2015), we performed a standard kinematic decomposition of the stellar component in the galaxies to determine the fraction of stars in each galaxy which are on planar circular orbits, and which are associated with a bulge (see also Vogelsberger et al. 2014; Tenneti, Mandelbaum & Di Matteo 2016). We note that this technique is not sensitive to the clumpiness of discs. This provides kinematically classified discs and bulges and a Disc to Total (D/T) ratio for our galaxy sample above a mass of total mass $10^{10}\,\mathrm{M}_\odot$ (which contains an appropriate number of stellar particles for this decomposition to be carried out). In particular, we follow Abadi et al. (2003) and define for every star particle with specific angular momentum j_z around a selected z-axis a circularity parameter $c = j_z/j(E)$, with $j(E)$ being the maximum specific angular momentum possible at the specific binding energy E of the star. Given c, as in standard practice in recent hydrodynamic simulations (Vogelsberger et al. 2014; Tenneti et al. 2016), we take disc particles with circularity $c > 0.7$ to be in the disc component. We then calculate the D/T for the stellar component of each galaxy. Based on those values, we can split galaxies into different types, discs and bulge/spheroid dominated. Consistent with previous work, here we use a threshold of D/T > 0.3 to classify a galaxy as disc-dominated.

Here, we also add a calculation of the large-scale tidal field. The tidal field can be characterized by three eigenvalues of the local tidal tensor, t_1, t_2 and t_3 (by definition $t_1 > t_2 > t_3$) and the corresponding eigenvectors $\boldsymbol{t}_1, \boldsymbol{t}_2$ and $\boldsymbol{t}_3$. The three eigenvalues satisfy $t_1 + t_2 + t_3 \equiv 0$ so that t_1 is always positive and t_3 is negative. Thus, the tidal field stretches material along t_1 and compresses material along t_3. By using t_1 as the indicator of the local tidal field strength we are following standard usage. We define the tidal field as the trace-less part of the strain tensor

$$T_{ij} = S_{ij} - \frac{1}{3}\sum_i S_{ii}, \tag{1}$$

where the strain tensor S_{ij} is the second derivative of the potential ϕ,

$$S_{ij} = \nabla_i \nabla_j \phi. \tag{2}$$

The large-scale strain tensor is calculated in Fourier space, following the procedures in Dalal et al. (2008):

$$\hat{S}_{ij} = \frac{k^2}{k_i k_j}\hat{\delta}. \quad (3)$$

A uniform 1/1000th sub-sample of the BlueTides particles is assigned to a mesh of 512 grid points per side using a Cloud-in-Cell assignment scheme (Hockney & Eastwood 1981). The density field is smoothed by a Gaussian window $\exp(-0.5\,k^2\,s^2)$ with a width of $s = 1$, 2 and $5\,h^{-1}$Mpc. The strain tensor value on the mesh is re-sampled at the location of the central BH particles using Cloud-in-Cell interpolation. We note that our definition is different from that of Wang et al. (2011), where the calculation is performed in configuration space using the nearest neighbour galaxies.

3 RESULTS

3.1 The early assembly of the most massive BHs

We turn directly to the population of the most massive BHs in BlueTides and their host galaxies. The left-hand panel of Fig. 1 shows BH mass versus stellar mass of the host galaxies at $z = 8$ (for galaxies with a BH that is more than five times the seed mass). The colours of the points indicate the D/T ratio for the stellar component of each galaxy. The most massive BH in BlueTides has a mass of $4 \times 10^8\,\mathrm{M}_\odot$ at $z = 8$. Interestingly, this most extreme BH does not appear to be hosted by the largest galaxy, in terms of stellar mass, and it has a significantly more dominant spheroidal component (D/T only 0.2) than most of the more massive galaxies Feng et al. (2015). The most massive BH is (positively) offset from the main $M_{\rm BH} - M_*$ relation defined by the rest of the population indicating a relatively faster growth of the BH compared to the stellar host. There are five objects with $M_{\rm BH}$ approaching $10^8\,\mathrm{M}_\odot$, and only two of those in the most massive galaxies with D/T > 0.5 (see Fig. 6). A large fraction of the massive BH population (with $M_{\rm BH} \approx 10^8\,\mathrm{M}_\odot$) is hosted in intermediate stellar mass galaxies with relatively dominant spheroidal components. Examining the left-hand panel of Fig. 1, we can see that both the orange points (spheroids) and blue points (discs) follow a relationship between stellar mass and BH mass, but that the locus of the spheroid-dominated galaxies is above (higher BH mass) the discs.

Looking at the BH accretion rates (right-hand panel of Fig. 1), we can see that the largest BH accretion rates are also typically found in the BHs hosted in the more spheroidal galaxies. The locus of BH accretion rate versus stellar mass for the spheroids is also displaced towards higher BH mass. In summary therefore, for a given stellar mass, the majority of the most massive BHs seen at $z = 8$, and those accreting at the largest rates, appear to be hosted by [extremely compact (half-light radii between 0.5 and 1 kpc); Feng et al. 2015 spheroid-dominated galaxies. In Feng et al. (2015), we discussed the population of massive galaxies with significant disc components.

3.2 Examples of high-z massive BHs

3.2.1 Environments

To illustrate the environments and corresponding host galaxy morphologies of the most massive BHs, we show in Fig. 2 images of 3 regions containing the most massive BHs in the simulation at $z = 8$. In Fig. 3, we compare the environments and hosts of the most massive BH in BlueTides (with $M_{\rm BH}\,4 \times 10^8\,\mathrm{M}_\odot$) with that of one

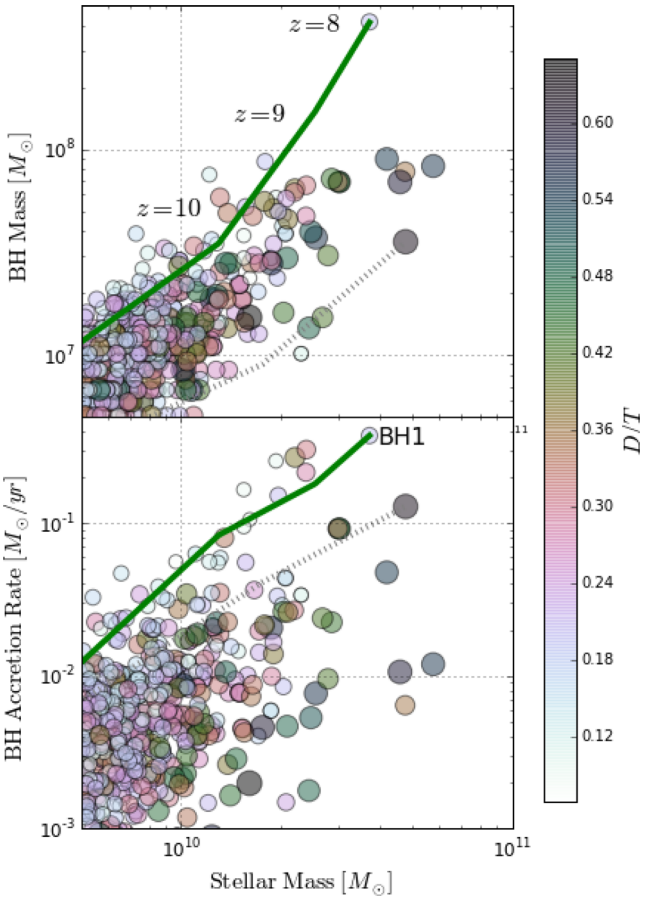

Figure 1. Top panel: black hole mass versus host galaxy stellar mass at $z = 8$. Colours indicate the disc-to-total (bulge plus disc) ratio for the stellar component, so that blue colours indicate discs and yellow/orange spheroid-dominated hosts. The most massive black hole at $z = 8$ in BlueTides has a mass of $M_{\rm BH} = 4 \times 10^8\,\mathrm{M}_\odot$ and resides in a spheroidal host. There are about half a dozen black holes with masses close to $10^8\,\mathrm{M}_\odot$. The green and dashed tracks show the redshift evolution of the most massive BH and a massive disc in this plane, both shown in Figs 3 and 4. The size of the symbols indicates the size of the galaxies, in particular, it represents the half-mass radius (ranging from sub kpc up to a few kpc) of the galaxies as measured in Feng et al. (2015).

of a representative massive disc, with D/T = 0.6, as discussed in Feng et al. (2015) (to be specific, we have chosen one of the most massive ones, also shown in fig. 1 of Feng et al. 2015). The basic properties of the four most massive black holes (in Figs 2 and 3) are summarized in Table 1. For both figures, the images show the projected gas density after zooming into scales 6, 3 and $0.5\,h^{-1}$ Mpc on a side (for the left, centre and right images in each set, respectively). The final inset in the right-hand panel shows the central galaxy host (adaptively smoothing the star particle distribution and colour coding according to stellar age). The positions of the BHs in all images are indicated with white crosses, the sizes of which are proportional to BH mass. It is interesting to note that only one of these massive BHs is close to undergoing a major merger, and all other massive BHs appear to be associated with isolated high-density regions. These images suggest that the most massive BHs may favour quasi-spherically collapsed regions of the density field and, in turn, that such environments are more conducive to the formation to spheroid dominated systems rather than disk-dominated stellar hosts. We will investigate this further in Section 4. The

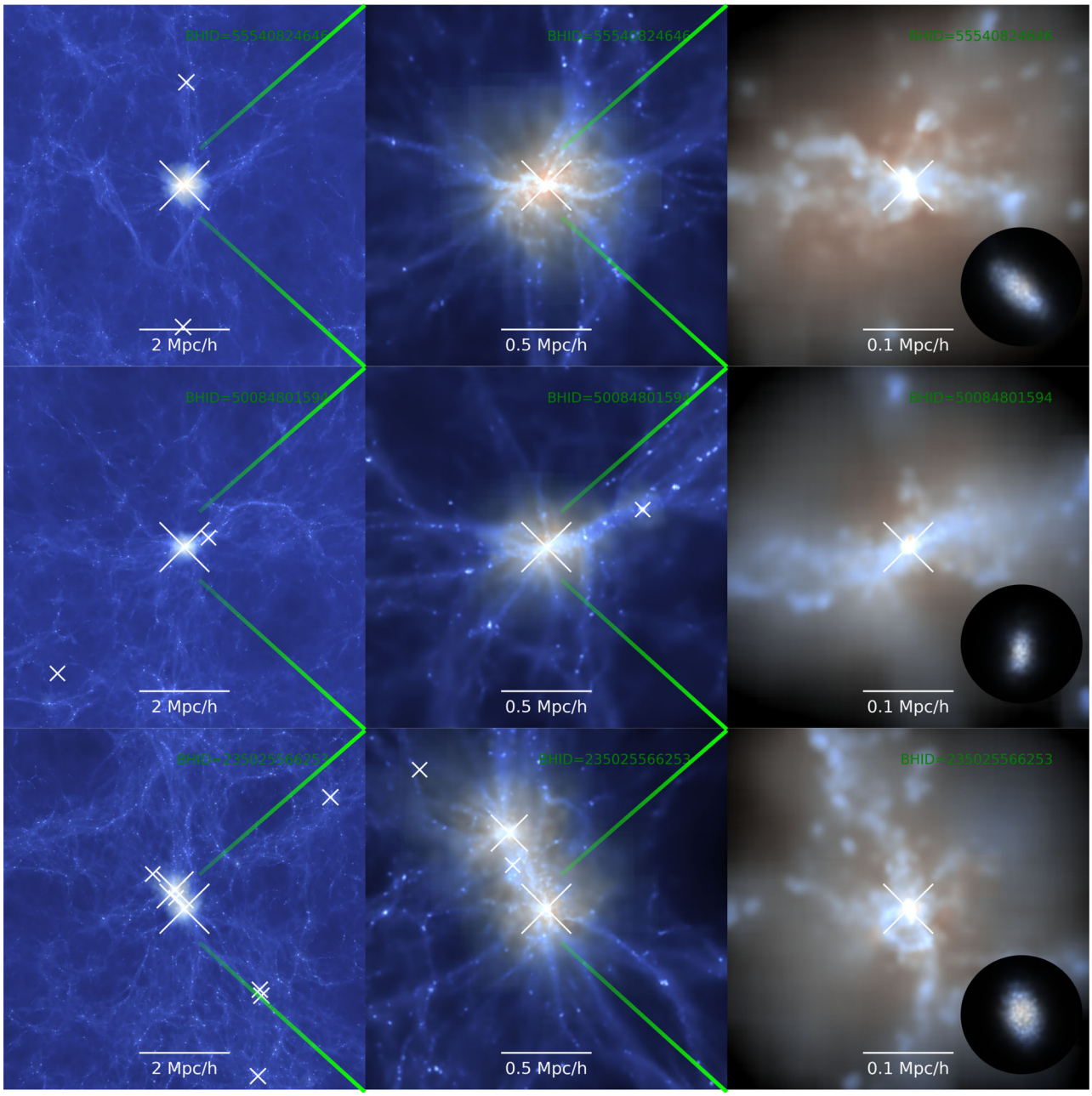

Figure 2. The environments of the most massive $z = 8$ black holes in BlueTides. The images show the large-scale gas density around the black holes, zooming into regions of width 6 (left-hand panels) to 3 h^{-1} Mpc (centre panels) and 0.5 h^{-1} Mpc (right-hand panels). The gas density field is colour coded by temperature (blue to red indicating cold to hot, respectively). The final zoom in the top right column shows the stellar density for the host galaxy, colour coded by stellar age. The positions of the black holes in all images are indicated with white crosses, the sizes of which are proportional to black hole mass. From top to bottom, these are BH2, BH3 and BH4 in Table 1.

massive ($M_* > 10^{10}\,M_\odot$) disc-dominated galaxies (chosen to have the highest D/T ratios and above the threshold value of D/T = 0.3) also host BHs, but generally have a wide range of BH mass at these epochs (and also are not hosting the most massive BH). We quantify the origin of the massive galaxy morphology and related BH growth in Section 3.3.

3.2.2 *Evolution*

In this section, we study the evolution of a number of properties for the most massive BHs and for illustration purposes, compare them to those of those of the diskiest (highest D/T ratio) massive stellar systems ($M_* \geq 10^{10}\,M_\odot$.) Fig. 4 shows the co-evolution from $z = 12$ to 8 of BH mass and stellar mass for the sample of the four most massive BHs at $z = 8$ shown in Figs 2 and 3 (solid lines). Each line represent a single BH as it moves from the lower left region and ends up in the top right. The x-axis is the corresponding stellar mass of its host galaxy. For comparison, the dashed lines show the tracks for four other BHs, which reside in some disc-dominated hosts (one of which is shown in the top panel of Fig. 3). The tracks of BH mass versus stellar mass are steeper for the most massive BHs indicating a relatively faster BH growth than host stellar mass

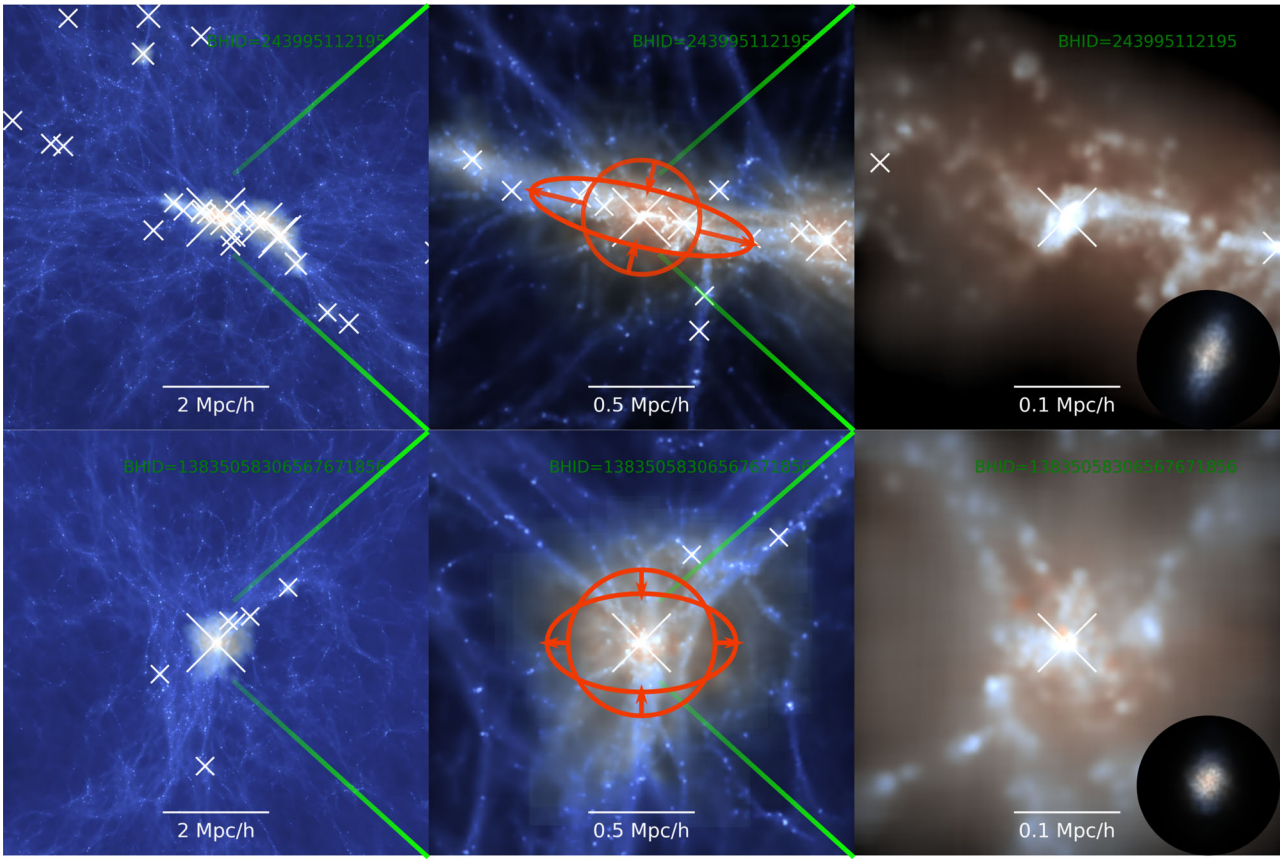

Figure 3. Same as Fig. 2. The environment of the most massive disc galaxy (D/T >0.3, top row) compared to that of the host galaxy of the most massive black hole (bottom row). The orange ellipses and arrows represent the tidal field t_1 and t_3 in the two cases. Tidal fields stretch material along t_1 and compress material along t_3. Strong tidal fields, meaning large t_1 values are found in the large-scale filament in the environment of the disc galaxy and small t_1 and associated thin, 'cold' filaments are characteristic of the environments of the most massive BHs. The most massive black hole is BH1 in Table 1.

Table 1. Basic properties of the four most massive black holes and their hosts at $z = 8$. Images of the environments and host galaxies of these objects are shown in Fig. 2.

Property	BH1	BH2	BH3	BH4
$M_{\rm BH}(\times 10^8\,{\rm M}_\odot)$	4.1	0.9	0.9	0.8
$M_{200}(\times 10^{10}\,{\rm M}_\odot)$	42	33	44	92
$M_{\rm star}(\times 10^{10}\,{\rm M}_\odot)$	3.7	2.5	4.1	5.7
$M_{\rm gas}(\times 10^{10}\,{\rm M}_\odot)$	4.0	3.9	4.9	13
$f_{\rm gas}[M_{\rm gas}/(M_{\rm gas}+M_{\rm star})]$	0.5	0.6	0.6	0.7
$r_{1/2}$ (kpc)	0.7	0.8	0.5	0.9
D/T	0.2	0.2	0.5	0.5
t_1 (tidal field)	0.29	0.23	0.32	0.08

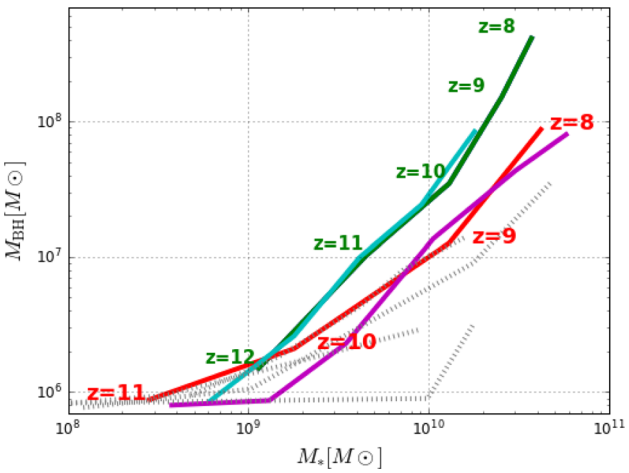

Figure 4. The co-evolution of black hole mass and stellar mass in the four most massive black holes (solid lines) compared to the four highest D/T galaxies (dashed lines).

growth compared, for example, to the most disc-dominated systems. The latter tend instead to grow in stellar mass relatively faster than in BH mass (moving mostly along the x-axis in this plane). At this early time, a very rapid phase of BH growth is required in order to explain the extremely massive rare objects that are seen. This rapid growth is consistent with the BH leading galactic growth through early assembly.

Fig. 5 tracks directly the evolution of the BH mass and accretion rate for the four most massive BHs (solid lines) and those of the disciest, massive stellar systems. As expected, the BHs that build up the largest masses accrete close to their critical Eddington accretion rate almost the entire time since they were seeded. Note, however, that the BHs are not exclusively following the Eddington rate but show some variability, with peaks and troughs while remaining close to that value. These are a result of the complex interplay of an AGN feedback and gas flow. While feedback is unable to quench and completely heat and remove the accreting gas, the inflows are disturbed and the accretion rate has significant variations particularly towards lower redshifts ($z \sim 8$). In the left-hand panel of Fig. 5, we can see that at this epoch BH mass is still growing steeply, with no sign that it has saturated at its final value. This is consistent with

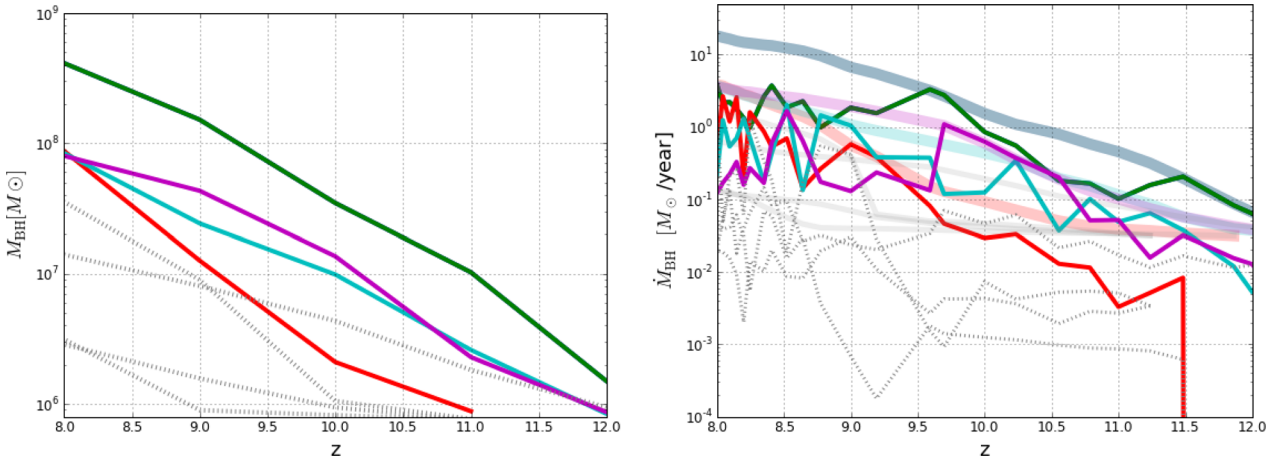

Figure 5. The evolution of black hole and accretion rate (left- and right-hand panel, respectively). Solid lines: black hole mass and corresponding accretion rate for the most massive black holes at $z = 8$. Dashed lines: a sample of the black holes in the most disc-dominated galaxies at $z = 8$. Right-hand panel: the thick shaded solid lines so the corresponding Eddington accretion rate values.

observations of SDSS quasars which have implied masses close to $10^9\,M_\odot$ at $z \sim 6$ (Di Matteo et al. 2012, see also). From the right-hand panel of Fig. 5 we can see that the BH accretion rates in disc-dominated objects are about an order of magnitude lower than in the most massive BH sample.

In Fig. 6, we turn to the evolution of the associated D/T ratio and SFR of the host galaxies of the massive BHs and massive discs discussed in Fig. 5.

We have seen (Figs 1 and 2) that at fixed stellar mass, galaxies with higher BHs tend to be more spheroid-dominated. Fig. 6 shows that indeed the D/T ratios are smaller for the hosts of massive BHs than the diskiest massive objects shown here (by construction the comparison sample has the highest values of D/T at $z = 8$) and in particular that D/T generally stays small with redshift (at least over the redshift range we can access with BlueTides). Note however, that in two of the examples shown the D/T is around 0.5. These objects are therefore not formally spheroid dominated and some of the massive BH object do retain/build up a somewhat significant disc component. There is obviously a large scatter in these properties and we will make use of the full statistical population (c.f. Section 3.3) of BHs and discs. Finally, the measurement of D/T becomes somewhat more uncertain towards the highest redshifts due to the smaller stellar masses of galaxies at earlier times. It is also interesting to note that while the typical SFRs are pretty high at the highest redshifts for the massive BHs in the spheroid-dominated hosts, they do not increase by much at lower redshifts probed here. For the disc-dominated massive hosts on the other hand, the star formation rates increase rapidly, reaching up to several $1000\,M_\odot\,yr^{-1}$, factors of 50 or more higher than in the massive BH hosts. It appears therefore that the presence and fast growth of a massive BH in these early compact spheroids is able to quench (through its associated feedback) the SFR in the massive BH hosts. This somewhat evident also in Fig. 2, where the stellar population in the central region of the spheroid is rather old (shown by the ref colours). We note however even in these high-z gas rich environments the SFR are still a few hundred $M_\odot yr^{-1}$.

3.3 The origin of the fastest BH growth: tidal field strength

Our results so far suggest that the growth of the most massive, early BHs in BlueTides is linked to mechanisms operating on and related to the formation of their hosts and not to the occurrence of major mergers. It also appears that the galaxy morphology at these epochs is related to BH growth. Whether a galaxy is disc-like or spheroid is likely imprinted early on (note however the relatively short time-scale probed in this study). These considerations and the visual differences in the large-scale distribution of surrounding matter (illustrated by Fig. 3) in regions surrounding host galaxies with rapid BH growth versus regions inducive of early disc formation suggest that net angular momentum and the impact of tidal field strength in these regions may play a role. In particular, we see that the large-scale distribution of the gas around the massive BHs is typically composed of thin, distinct filaments which do not interact and which lead to fast 'cold' gas accretion to prevail forming a spheroid host. The formation of spheroids in these environments has been seen in earlier work (Sales et al. 2012). In that work, the authors also suggested that galaxy morphology was related to spin alignment of accreting matter: The coherent alignment of the net spin and hence similar angular momentum leads to disc-dominated systems, whereas the direct filamentary accretion of cold gas is accompanied by spin misalignments and favours the formation of spheroids.

Along these lines, here we study the relation between the tidal field and spheroids with early massive BHs and the suppressed early growth of BHs in regions of disc formation. As an illustration, we show that, indeed, where tidal fields are large ($t_1 = 0.6$), a large-scale filament forms (see Fig. 3). This induces significant tangential motion in the accreting gas, leading to high angular momentum and the formation of a massive early disc. Conversely, the tidal field strength is low ($t_1 = 0.2$) in regions with thin converging filaments, which bring in cold material fast and lead to the formation of the most massive BH in a spheroid-dominated host.

We now move on from these illustrative examples to investigate whether these results also apply statistically to the galaxy morphology and BH accretion rates of the entire sample of massive galaxies in BlueTides. We measure the tidal field strength for the 22156 galaxies with stellar masses $>10^8\,M_\odot$) that host a BH at $z = 8$. In Fig. 7, we plot the mean D/T ratio and Eddington accretion rate as a function of the tidal field strength t_1 (measured at a scale of 1 Mpc)

We can see in the left-hand panel of Fig. 7 that the mean D/T ratio for the galaxies in BlueTides does show strong dependence on tidal

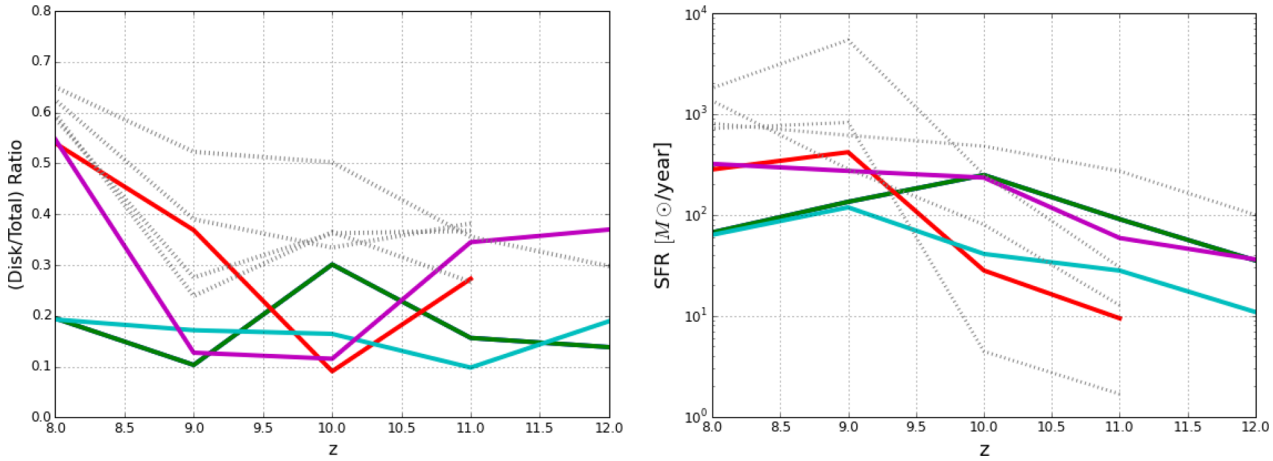

Figure 6. The D/T ratio for the host galaxies for black holes in Fig. 5. The solid lines and dashed lines correspond to those in Fig. 5.

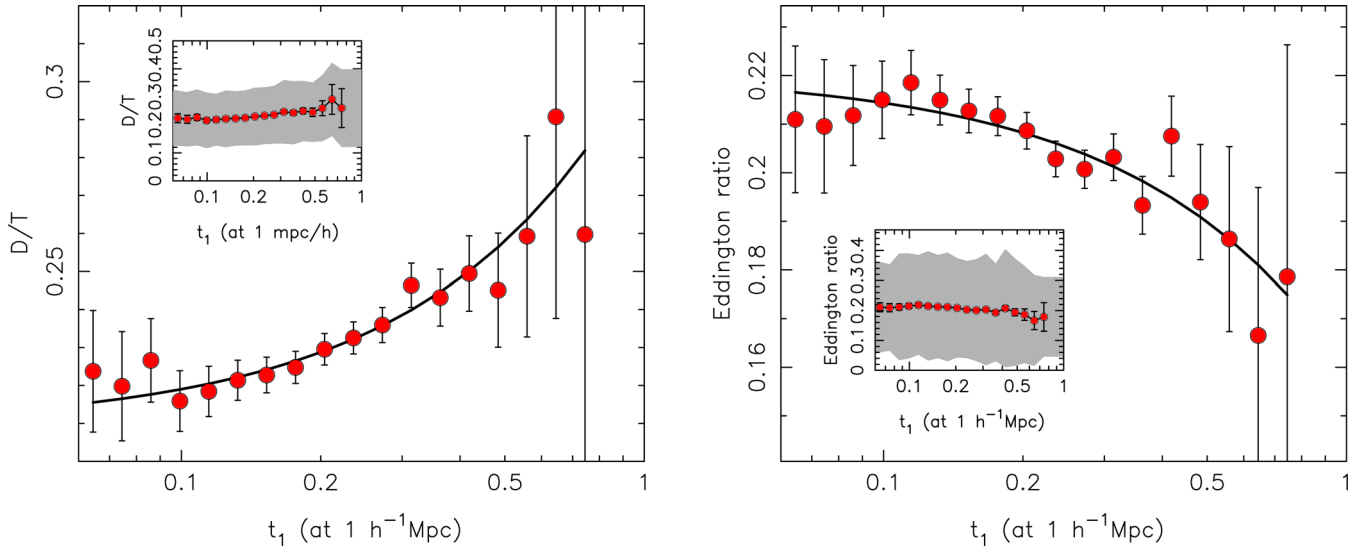

Figure 7. Left-hand panel: The disc-to-total ratio for BlueTides BH host galaxies versus t_1, the tidal field strength. Right-hand panel: the Eddington accretion rate of BHs versus t_1. The inset panels in each case show the same data, but with an increased y-axis range. The points with error bars show the mean values of D/T and Eddington ratio in bins of t_1. The error bar is the standard error of the mean and the shaded regions indicate the range which encloses 68 per cent of the galaxies in each bin. The smooth curves are linear fits of D/T and Eddington ratio to t_1, with the fit parameters given in Table 2.

field strength. As seen in the examples above, the high tidal field environments induce coherent acquisition of angular momentum and hence disc formation. Conversely, in the right-hand panel of Fig. 7 we find that on average, the largest BH accretion rates are induced in regions with the smallest tidal fields. This is consistent with the fastest BH growth at these early times being associated with those regions in which gas is accreted cold and fast through direct filamentary accretion. The most massive BHs thus may form even in the absence of mergers.

We quantify these relationships in two fashions. First, we compute the Spearman rank correlation coefficient r_s between t and D/T ratio and between t and Eddington accretion rate. We find $r_s \sim 0.1$ and $r_s \sim -0.05$, respectively, with very high significance (see the results in Table 2) This indicates that although there is scatter about the relation, there is an extremely significant correlation between t and D/T and an anticorrelation between t and accretion rate. We have also fit a simple linear relation between the values of D/T averaged in bins of t. A linear fit to the Eddington accretion values in bins of t is also acceptable. The parameters for these fits are also given in Table 2. The fits are to the mean D/T ratio and mean accretion rates averaged in t_1 bins (i.e. fits to the points plotted in Fig. 7). We have also tried computing a straight line fit directly to the cloud of 22 156 points representing each galaxy. In this case, we find that the fit parameters are similar, (e.g. for Eddington accretion rate versust_1 we find $a = 0.22$, $b = 0.066$ $\sigma_b = 0.012$) and the correlation is detected at slightly higher significance in each case

Table 2. Parameters a and b for a linear fit, $y = a + bx$ to the mean correlations between D/T ratio and BH Eddington accretion rate versus tidal field strength t_1 shown in Fig. 7, and versus local density ρ shown in Fig. 8. Also give the error bar on the fit parameter b, σ_b. The last two values in each row are the spearman rank correlation coefficient r_s and Δ the two sided significance of its deviation from zero. Here, small values indicate more significant correlations.

Property	a	b	σ_b	r_s	Δ
Galaxy D/T versus t_1	0.21	0.099	0.016	0.087	1.4×10^{-38}
BH Eddington versus t_1	0.22	−0.063	0.016	−0.049	1.78×10^{-13}
Galaxy D/T versus ρ	0.21	0.0217	0.0033	0.175	0
BH Eddington versus ρ	0.22	0.0057	0.0036	0.029	1.68×10^{-5}

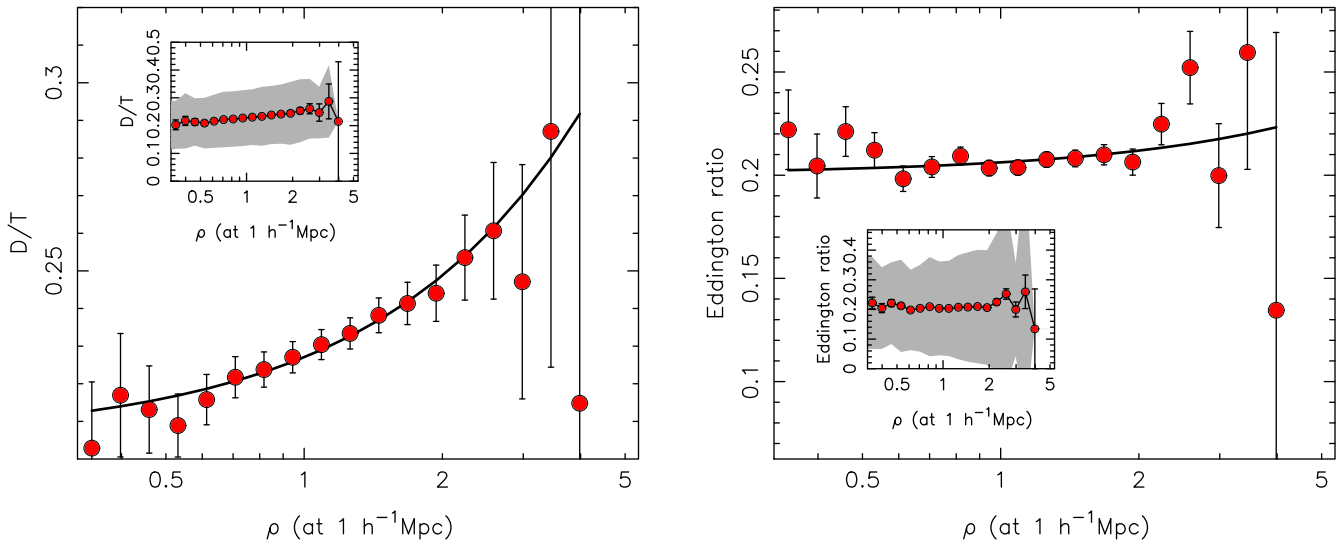

Figure 8. Left-hand panel: The disc-to-total ratio for BlueTides BH host galaxies versus ρ, the density (in a 1 Mpc h^{-1} radius sphere) in units of the cosmic mean. Right-hand panel: the Eddington accretion rate of BHs versus ρ. The inset panels in each case show the same data, but with an increased y-axis range. The points with error bars show the mean values of D/T and Eddington ratio in bins of ρ. The error bar is the standard error of the mean, and the shaded regions indicate the range which encloses 68 per cent of the galaxies in each bin. The smooth curves are linear fits of D/T and Eddington ratio to ρ, with the fit parameters given in Table 2

($b/\sigma_b = 0.066/0.012 = 5.5\sigma$ in this case, compared to 4σ for the fit to the mean).

We can compare these tidal field results to the effect of the local environmental density on the D/T ratio of galaxies and on the BH accretion rate. We have computed the density ρ on the same 1 Mpc h^{-1} scales as for t_1, and show the analogous plots in Fig. 8, where ρ is given in units of the cosmic mean. Linear fits to the relationship between D/T and ρ and accretion rate and ρ are also shown. We can see from the left-hand panel that there is, indeed, a strong dependence of D/T ratio on ρ, with disc galaxies inhabiting dense environments (a reversal of the usual morphology–density relation seen at $z = 0$). From Table 2, we can see that the significance of the relationship (σ_b/b) is approximately the same as that between tidal field and D/T ratio, indicating that they are both equally important for this quantity. The right-hand panel on the other hand shows that BH accretion rate is not as strongly correlated with local density as with tidal field. There is a hint that denser environments result in higher accretion rates, but this correlation is only significant at the $\sigma_b/b = 1.6\sigma$ level.

These quantitative results confirm our earlier suggestion that regions of significant tidal field strength hosting early massive galaxies preferentially lead to the formation of discs, while the lowest tidal fields lead on average to the more significant cold accretion and BH growth, and which is associated with the formation of spheroid-dominated systems.

4 CONCLUSIONS

We use the hydrodynamical cosmological simulation BlueTides to study the origin of the most massive BHs at early times. Here, we have focused our analysis on the massive galaxies and BHs at $z \geq 8$ (for earlier discussion of $z = 6$ SDSS quasars, see e.g. Di Matteo et al. 2012; Feng et al. 2014). In Feng et al. (2015), we discussed how the most massive galaxies at these epochs are likely disc dominated. Here, we have shown that while the most massive discs can still host massive BHs the most extreme early BH growth (reaching a M_{BH} a few $10^8\,M_\odot$ at $z = 8$) occurs in spheroid-dominated extremely compact galaxies. This is in line with Dubois et al. (2015), who also show that bulge formation (which is inhibited by SN feedback at early times) in high-z galaxies is mandatory to get the rapid growth of an SMBH. The sites of extremely rapid BH growth hosted by spheroid-dominated galaxies are the result of large-scale filamentary accretion of cold gas from which the halo and eventually BHs can accrete new material radially (at low angular momentum). The large scale, thin filamentary structures surrounding these haloes is a direct result of the relatively low tidal field strength due to the surrounding large-scale density field. In contrast, for haloes located in strong tidal fields, the surrounding filamentary structure is larger than the halo allowing material to be accreted from different directions producing more gradual accretion (deceleration along t_1) parallel to the large-scale filament – and acceleration (along t_3) – perpendicular to the filaments, allowing material to accrete angular momentum more coherently (see e.g. Sales et al. 2012).

We find that star formation rates, (in the selected sub-samples) of more spheroidal hosts and most massive BHs, are somewhat lower than in the disc dominated galaxies. The higher BH accretion rates in the former are responsible for driving strong BH feedback. We suggest (as supported by many previous studies) that AGN feedback is likely responsible for quenching the SFR in the inner regions and is hence conducive to the formation of a spheroidal (older star population) component. For selected (aassive) disc dominated hosts tend to have higher star formation rates. The SFRs in discy hosts arise after a gradual ramp up in time, while BH gas accretion rates tend to be more sub-Eddington (which leads to a much weaker influence of an AGN feedback) compared to the more spheroid-dominated hosts. We plan to explore the full analysis of the galaxy sample and their observational signatures of these populations of stars in the massive disc-dominated galaxies versus the most massive BH hosts in future work.

Our results suggest that a new scenario for the origin of the most massive early BHs, which does not rely on major gas rich mergers. This scenario offers clues to the origin of the most massive, rare high-z BHs. These extreme black holes can be grown at the

highest rates in high-density regions in the early Universe but not necessarily the most extreme ones: what is important is that they grow most rapidly in regions with relatively low tidal fields due to their environments. The fact that the brightest quasars at these early times host the most massive BHs, but do not necessarily have to live in the densest regions of the universe, implies that they are unlikely to be the precursors of the massive BHs in clusters of galaxies today. More likely their descendants will not be in privileged sites but in rather isolated galaxies (e.g. Thomas et al. 2016). Other recent observational studies (Ferré-Mateu et al. 2015) of extreme outliers from the $M_{\rm BH}$–$M_{\rm bulge}$ relation at the high-mass end also support the idea that the most massive have missed an accretion phase by mergers and have remained compact, massive and with spheroidal shapes.

Our work and the finding that BH growth is linked to tidal field theory offers some explanation as to the origin of the most massive BHs in the most compact galaxies. It is interesting that Barber et al. (2016) using the EAGLE simulation at $z = 0$ also found a strong link between compactness of the host and the most anomalously high BH mass outliers in the $M_{\rm BH}$–M_* relation. These authors also find that the most extreme outliers grow rapidly in $M_{\rm BH}$ at early times to lie well above the present-day $M_{\rm BH}$–M_* relation and are consistent with undisturbed morphologies implied by late time observations. In the context of our findings it is likely that, indeed, the most extreme massive BH outliers are linked to regions with lower tidal fields in the initial conditions. While it is currently unfeasible (with any current HPC) to run BlueTides to $z = 0$, we also plan to carry out a Dark-Matter-Only BlueTides, which will allow us to study the environments of the descendants of the earliest supermassive BHs (by tracing their history through their host haloes).

Our findings imply that the fastest BH growth is a direct consequence of the initial conditions of the density field. Although the limited time evolution and somewhat limited numerical resolution of the large volumes of BlueTides precludes more detailed studies and investigations, we plan to use these clues to re-simulate some of these systems at higher resolution (Feng et al. 2014, as we did with MassiveBlack simulation, see e.g.) with the goal of studying in more detail the dependence on different seed BH scenarios. In this context, it is promising that Pezzulli, Valiante & Schneider (2016), using semi-analytic models, have shown that similarly high BH masses ($\sim$ a few $\times 10^8\,{\rm M}_\odot$) at $z = 8$ are also consistent with small BH seeds ($\sim 100\,{\rm M}_\odot$) and with different accretion regimes. We note that (Danovich et al. 2015, and references therein) have studied in detail the angular-momentum build up in *high* $- z$ massive galaxies using high-resolution zoom cosmological simulations and have explicitly studied the link with early disc formation and tidal field theory. In our work, we illustrate that BH formation and angular momentum build up can be understood within the same context.

ACKNOWLEDGEMENTS

We thank Y. Dubois and M. Volonteri for early discussions on the importance of angular momentum build-up for early, massive BH formation. We acknowledge funding from NSF ACI-1036211, NSF ACI-1614853, NSF AST-1517593, NSF AST-1009781, NSF AST-1616168 and the BlueWaters PAID program. The BlueTides simulation was run on the BlueWaters facility at the National Center for Supercomputing Applications. SMW acknowledges support from the UK Science and Technology Facilities Council.

REFERENCES

Abadi M., Navarro J., Steinmetz M., Eke V., 2003, ApJ, 591, 499
Barber C., Schaye J., Bower R. G., Crain R. A., Schaller M., Theuns T., 2016, MNRAS, 460, 1147
Battaglia N., Trac H., Cen R., Loeb A., 2013, ApJ, 776, 81
Bouwens R. J. et al., 2015, ApJ, 803, 34
Chabrier G., 2003, ApJ, 583, L133
Dalal N., White M., Bond J. R., Shirokov A., 2008, ApJ, 687, 12
Danovich M., Dekel A., Hahn O., Ceverino D., Primack J., 2015, MNRAS, 449, 2087
Di Matteo T., Springel V., Hernquist L., 2005, Nature, 433, 604
Di Matteo T., Khandai N., DeGraf C., Feng Y., Croft R. A. C., Lopez J., Springel V., 2012, ApJ, 745, L29
Dubois Y., Pichon C., Haehnelt M., Kimm T., Slyz A., Devriendt J., Pogosyan D., 2012, MNRAS, 423, 3616
Dubois Y., Volonteri M., Silk J., Devriendt J., Slyz A., Teyssier R., 2015, MNRAS, 452, 1502
Fan X. et al., 2006, AJ, 132, 117
Faucher-Giguère C.-A., Lidz A., Zaldarriaga M., Hernquist L., 2009, ApJ, 703, 1416
Feng Y., Di Matteo T., Croft R., Khandai N., 2014, MNRAS, 440, 1865
Feng Y., Di Matteo T., Croft R., Tenneti A., Bird S., Battaglia N., Wilkins S., 2015, ApJ, 808, L17
Feng Y., Di-Matteo T., Croft R. A., Bird S., Battaglia N., Wilkins S., 2016, MNRAS, 455, 2778
Ferré-Mateu A., Mezcua M., Trujillo I., Balcells M., van den Bosch R. C. E., 2015, ApJ, 808, 79
Fioc M., Rocca-Volmerange B., 1997, A&A, 326, 950
Hinshaw G. et al., 2013, ApJS, 208, 19
Hockney R. W., Eastwood J. W., 1981, Computer Simulation Using Particles. McGraw-Hill, New York
Jiang L. et al., 2009, AJ, 138, 305
Katz N., Weinberg D. H., Hernquist L., 1996, ApJS, 105, 19
Krumholz M. R., Gnedin N. Y., 2011, ApJ, 729, 36
Mortlock D. J. et al., 2011, Nature, 474, 616
Nelson D. et al., 2015, Astron. Comput., 13, 12
Pezzulli E., Valiante R., Schneider R., 2016, MNRAS, 458, 3047
Sales L. V., Navarro J. F., Theuns T., Schaye J., White S. D. M., Frenk C. S., Crain R. A., Dalla Vecchia C., 2012, MNRAS, 423, 1544
Schaye J. et al., 2015, MNRAS, 446, 521
Song M. et al., 2016, ApJ, 825, 5
Springel V., Hernquist L., 2003, MNRAS, 339, 289
Tenneti A., Mandelbaum R., Di Matteo T., 2016, MNRAS, 462, 2668
Thomas J., Ma C.-P., McConnell N. J., Greene J. E., Blakeslee J. P., Janish R., 2016, Nature, 532, 340
Vogelsberger M., Genel S., Sijacki D., Torrey P., Springel V., Hernquist L., 2013, MNRAS, 436, 3031
Vogelsberger M. et al., 2014, MNRAS, 444, 1518
Wang H., Mo H. J., Jing Y. P., Yang X., Wang Y., 2011, MNRAS, 413, 1973
Waters D., Di Matteo T., Feng Y., Wilkins S. M., Croft R. A. C., 2016a, MNRAS, 463, 325
Waters D., Wilkins S., Di Matteo T., Feng Y., Croft R., Nagai D., 2016b, MNRAS, 461, L51
Wilkins S. M., Feng Y., Di-Matteo T., Croft R. D. W., 2016a, MNRAS
Wilkins S. M., Feng Y., Di-Matteo T., Croft R., Stanway E. R., Bouwens R. J., Thomas P., 2016b, MNRAS, 458, L6
Wilkins S. M., Feng Y., Di-Matteo T., Croft R., Stanway E. R., Bunker A., Waters D., Lovell C., 2016c, preprint (arXiv: e-prints)

This paper has been typeset from a TEX/LATEX file prepared by the author.